Atomic Force Microscopy Studies of Functional and Dysfunctional Pulmonary Surfactant Films, II: Albumin-Inhibited Pulmonary Surfactant Films and the Effect of SP-A

Yi Y. Zuo,*†‡ Seyed M. Tadayyon,* Eleonora Keating,* Lin Zhao,‡ Ruud A. W. Veldhuizen,§ Nils O. Petersen,*†¶ Matthias W. Amrein,‖ and Fred Possmayer†‡

*Department of Chemistry, †Department of Biochemistry, ‡Department of Obstetrics and Gynaecology, §Department of Physiology and Pharmacology and Department of Medicine, University of Western Ontario, London, Ontario, Canada; ¶National Institute for Nanotechnology, National Research Council of Canada, Edmonton, Alberta, Canada; and ‖Department of Cell Biology and Anatomy, University of Calgary, Calgary, Alberta, Canada

ABSTRACT Pulmonary surfactant (PS) dysfunction because of the leakage of serum proteins into the alveolar space could be an operative pathogenesis in acute respiratory distress syndrome. Albumin-inhibited PS is a commonly used in vitro model for studying surfactant abnormality in acute respiratory distress syndrome. However, the mechanism by which PS is inhibited by albumin remains controversial. This study investigated the film organization of albumin-inhibited bovine lipid extract surfactant (BLES) with and without surfactant protein A (SP-A), using atomic force microscopy. The BLES and albumin (1:4 w/w) were cospread at an air-water interface from aqueous media. Cospreading minimized the adsorption barrier for phospholipid vesicles imposed by preadsorbed albumin molecules, i.e., inhibition because of competitive adsorption. Atomic force microscopy revealed distinct variations in film organization, persisting up to 40 mN/m, compared with pure BLES monolayers. Fluorescence confocal microscopy confirmed that albumin remained within the liquid-expanded phase of the monolayer at surface pressures higher than the equilibrium surface pressure of albumin. The remaining albumin mixed with the BLES monolayer so as to increase film compressibility. Such an inhibitory effect could not be relieved by repeated compression-expansion cycles or by adding surfactant protein A. These experimental data indicate a new mechanism of surfactant inhibition by serum proteins, complementing the traditional competitive adsorption mechanism.

INTRODUCTION

The deficiency or dysfunction of pulmonary surfactant (PS) causes severe respiratory diseases. Neonatal respiratory distress syndrome (RDS), the major disease of PS deficiency worldwide, arises primarily from prematurity (1). It is estimated that RDS affects up to 10% of all premature infants in developed countries (2). In 2002, RDS affected an estimated 24,000 newborns in the United States alone (2). Displaying symptoms similar to those of RDS, acute lung injury (ALI) and its more severe form, acute respiratory distress syndrome (ARDS), exhibit a rapid onset of respiratory failure that can affect patients at any age (3). Acute respiratory distress syndrome affects ~150,000 people per year in the United States, and has a case fatality rate of 30–40% (4). The pathogenesis of ARDS is not fully understood, but surfactant dysfunction is believed to be an operative cause, induced by a primary pathogenesis such as extensive lung inflammation, trauma, severe pulmonary infection, oxygen toxicity, or radiation damage (5,6).

Exogenous surfactant replacement therapy, in which either synthetic or modified natural PS extracted from bovine or porcine sources is delivered into the patients' lungs, is established as a standard therapeutic intervention for newborns with RDS (7). Owing in part to surfactant therapy, the mortality rate of premature infants in the United States attributable to RDS fell by 24% in 1990, and has continued to decrease (8,9). Inspired by their symptomatic similarity, surfactant therapy was also attempted in the treatment of ARDS (10). However, this has achieved limited success to date (11,12). It was proposed that surfactant inactivation is partially responsible for this unsatisfactory performance (5,6,11,13).

Surfactant inhibition (inactivation or dysfunction) refers to those processes that decrease or abolish the normal biophysical properties of PS (1,14). Such processes may 1), interfere with phospholipid (PL) adsorption to form a functional film that decreases surface tension to 20–25 mN/m, 2), prevent the film from reaching low surface tensions (<5 mN/m) upon compression, or 3), impair the readsorption or reinsertion of PL vesicles during expansion (14). A number of substances were reported to inhibit PS, including serum proteins, unsaturated membrane PL, lysophospholipids, unsaturated free fatty acids, meconium, and supraphysiological levels of cholesterol (1,6,13–15).

In vitro biophysical studies established two distinct inhibition mechanisms: inhibition attributable to serum proteins via competitive adsorption, and inhibition attributable to unsaturated and other lipids through mixing with and fluidizing otherwise stable PL films (14,16). The competitive adsorption

Submitted February 2, 2008, and accepted for publication May 14, 2008.

Address reprint requests to Fred Possmayer, Dept. of Obstetrics/Gynaecology, Schulich School of Medicine and Dentistry Dental Sciences, Building 5009, University of Western Ontario, London, Ontario N6A 5C1, Canada. Tel.: 519-661-2111, ext. 80972; Fax: 519-661-3175; E-mail: fpossmay@uwo.ca.

Editor: Thomas Schmidt.

0006-3495/08/09/2779/13 $2.00

doi: 10.1529/biophysj.108.130732

mechanism stipulates that surface-active serum proteins, such as albumin and fibrinogen, compete with PL for space at the air-water interface. This inhibition mechanism was first proposed by Holm et al. and by Tabak and Notter, based on early studies of surfactant inhibition using the Langmuir-Wilhelmy balance (LWB) and the pulsating bubble surfactometer (PBS) (16–19). These authors found that PS adsorption was inhibited when mixed with albumin before exposure to an air-water interface. When the adsorption barrier was removed either by spreading PS on top of an albumin-containing subphase (19), or by spreading PL and albumin alternately at the air-water interface (17), no inhibitory effects were found. These tensiometric studies suggested that albumin and other serum proteins, when present in the subphase, can inhibit PS by adsorbing more rapidly to the air-water interface. Once adsorbed, the protein molecules exclude PL vesicles from entering the interface by creating a steric or electrostatic energy barrier (20,21). This inhibition mechanism was proven to be operative, at least in vitro, by directly imaging PL adsorption in the presence of albumin, using Brewster angle microscopy (20) and fluorescence microscopy (22,23). In keeping with this view, low-concentration surfactant injected under preadsorbed albumin films, or mixed with albumin in the subphase, adsorbs slowly (19,20,24,25). Also consistent with competitive adsorption is the experimental observation that inhibition attributable to serum proteins can be overcome by increasing surfactant concentration (16), by adding surfactant protein A (SP-A) (26–28), or by adding carbohydrate polymers (20,21,23,25,29). These approaches enhance the adsorption rate of the PL vesicles of PS, and thus overcome serum protein competition for the air-water interface.

Despite its success in interpreting in vitro inhibition of PS by albumin and other serum proteins, the relevance of the competitive adsorption mechanism to ARDS remains uncertain. Indeed, leakage of serum proteins into the alveolar space because of an impaired blood-air barrier is an early event in the pathogenesis of ARDS (13). However, the levels of these serum proteins relative to surfactant PL in the alveolar lining layer of injured lungs are not unambiguously established. Biophysical studies in vitro demonstrated that with surfactant levels of 3 mg/mL, no obvious inhibitory effects were noted with even eightfold greater albumin levels (16). It was also found that the adsorption or spreading of high-concentration PS (i.e., 27 mg/mL) was not significantly inhibited, even in the presence of high-concentration albumin (30).

More recent studies on surfactant PL bilayers and monolayers provided evidence that molecular interactions or binding between PL and serum proteins may contribute to surfactant inhibition (31–33). These suggestions are consistent with the views of Seeger et al. during early studies of surfactant inhibition (34). These authors demonstrated that fibrin, generated from fibrinogen, inhibited surfactants from attaining low surface tensions by forming insoluble complexes, thus suggesting specific interactions between fibrin and PL in these surfactants.

The effect of SP-A in overcoming surfactant inhibition because of serum proteins is also unclear. Surfactant protein A is absent from all therapeutic surfactant preparations currently on the market. It is known that adding SP-A to lipid extract surfactants in vitro increased their resistance to inhibition because of serum proteins (26–28) and meconium (28). In animal experiments, surfactants containing SP-A showed higher resistance to inhibition than those without SP-A (28,35–37).

Here, we studied albumin-inhibited bovine lipid extract surfactant (BLES) films with and without SP-A, using atomic force microscopy (AFM). Albumin and BLES were cospread at the air-water interface of a LWB from aqueous media. Cospreading minimized (if not completely eliminated) the adsorption barrier imposed by preadsorbed albumin molecules on PL vesicles, i.e., inhibition attributable to competitive adsorption. It was found that BLES films were significantly inhibited by the cospread albumin, as indicated by increased film compressibility. This inhibition was not mitigated by repeated compression-expansion cycles. AFM revealed variations in film organization from a surface pressure (π) of 20–40 mN/m, compared with pure BLES monolayers. These variations were attributable to albumin molecules that remained at the interface and mixed with the BLES films, as revealed by fluorescence confocal microscopy. It was also found that adding SP-A did not counteract the inhibition because of cospread albumin, which indicates a primary role of SP-A in reversing inhibition by enhancing PL adsorption. These experimental data may indicate a new mechanism of surfactant inhibition because of serum proteins, and may have implications in the further development of surfactant therapy for treating ARDS.

MATERIALS AND METHODS

Materials

The BLES (BLES Biochemicals, London, Ontario, Canada) and human SP-A were described in detail previously (38). Briefly, BLES contains all of the PL in natural surfactant and hydrophobic surfactant proteins (SP-B and SP-C), whereas it is devoid of hydrophilic surfactant proteins (SP-A and SP-D) and cholesterol. The BLES was diluted to 5 mg/mL, using a saline buffer of 0.9% NaCl, 1.5 mM $CaCl_2$, and 2.5 mM HEPES at pH 7.0. The SP-A was added to BLES at 2.5% relative to the weight of PL in the BLES.

Bovine serum albumin (BSA) (minimum 99%, essentially globulin and fatty acid-free) and fluorescein isothiocyanate (FITC)-labeled BSA were purchased from Sigma Chemical Co. (St. Louis, MO) and used without further purification. An albumin concentration of 20 mg/mL was used. This concentration is approximately half of the albumin concentration in serum, and is close to the average albumin concentration in the alveolar fluid of ARDS patients as reported by Ishizaka et al. (39).

Langmuir-Wilhelmy balance

The spreading, compressing, and Langmuir-Blodgett (LB) transfer of surfactant films was conducted in an LWB (μ-Trough, Kibron, Helsinki, Finland) at room temperature (24 $\pm$ 1°C). This trough contains a ~90 mL subphase, and has an operational surface area of ~125 cm^2. Detailed de-

scriptions of the experimental procedures can be found elsewhere (38). Briefly, cospreading BLES and albumin was achieved by depositing tiny droplets of aqueous mixtures of 5 mg/mL BLES, with and without 2.5 wt % SP-A, and 20 mg/mL BSA, uniformly throughout the air-water interface. For the sake of comparing film compressibility, the amounts of spread PL were the same as those for preparing BLES films without albumin (38), i.e., 20 μL for BLES-albumin without SP-A (containing 100 μg PL), and 10 μL for BLES-albumin with SP-A (containing 50 μg PL). It was shown that with the addition of SP-A, smaller amounts of spread PL were required to reach the same π (38).

It should be noted that when spread from aqueous media, it is possible for some PL vesicles to penetrate the air-water interface, instead of directly spreading, and to adsorb back with time. Therefore, cospreading BLES and albumin at the air-water interface cannot completely eliminate the process of competitive adsorption. However, taking into account the extremely small volumes of spreading and the relatively large volume of subphase, the chance that surface active material lost in the subphase readsorbs to the interface is small (40). Hence, the amount of material that is finally retained at the interface would largely depend on the initial incorporation/adsorption efficiency (40). Our previous studies showed that aqueous BLES samples at the studied concentration (i.e., 5 mg/mL) have a high adsorption efficiency (38). This is likely because of the high PL concentration, the hydrophobic surfactant proteins in BLES (SP-B/C), and the procedure of spreading from the airside, which minimizes the thermodynamic barrier for PL vesicles ''unzipping'' in water (14,41). Adsorption of BLES would be enhanced further by the addition of SP-A (38). Consequently, the effect of competitive adsorption in the cospread BLES-albumin films would be expected to be relatively small.

The spread films were compressed at a rate of 30 mm^2/s, i.e., at 0.24% of initial area per second. Because the exact amount of material at the interface is unknown, isotherms were expressed as the percentage of the initial area. The films at the air-water interface were transferred to freshly cleaved mica surfaces at π of 20, 30, 40, and 45 mN/m, at a rate of 2 mm/min, using the LB technique. The transfer ratios at π above 20 mN/m are much greater than 1, likely arising from losses of monolayer materials because of the collapse of albumin monolayers (at 30 and 40 mN/m) and PL monolayers (at 45 mN/m). For fluorescence imaging, BLES-albumin (1:4 w/w) films with 1% FITC-BSA were deposited at 30 mN/m onto glass coverslips.

Atomic force microscopy

Topographical AFM images were obtained using a Nanoscope III scanning force multimode microscope (Digital Instruments, Santa Barbara, CA) within 2 h of deposition. Samples were scanned with a J-type scanner, using the contact mode in air. A silicon nitride cantilever with a spring constant of 0.12 N/m was used. The scan rate was 1 Hz, and the force exerted on the samples was set at ~10 nN by adjusting the deflection setpoint. Section, roughness, and grain analyses of AFM images were performed using Nanoscope III software (version 5.12r3, Digital Instruments). Scion Image (Scion, Frederick, MD) was used to quantify the areas and sizes of domains in the AFM images. Quantification results are presented as average ± SD, calculated by analyzing multiple frames of different samples at different resolutions.

RESULTS

BLES with albumin

Fig. 1 shows the spreading (Fig. 1 *A*) and compression (Fig. 1 *B*) isotherms of BLES-albumin (1:4 w/w) films. (A compression isotherm of a representative pure BLES film is also shown in Fig. 1 *B* as a reference. For reasons of comparison, this isotherm is shifted to the right to coincide with the onset of compression isotherms of BLES-albumin films.) Spreading 20-μL samples (i.e., 100 μg BLES + 400 μg albumin) quickly increased π to an equilibrium value of ~20 mN/m, corresponding to the equilibrium spreading pressure (π_e) of albumin (22,25,42). Compared with BLES films formed by the same amount of PL (Fig. 1 *B*), the cospread BLES-albumin films show higher film compressibility ($Cm = -(1/A)(dA/d\pi)$). As summarized in Table 1, the compressibility of BLES-albumin films is nearly fivefold that of BLES films at 20 mN/m. The compressibility decreases with increasing π, and approaches the compressibility of BLES films at 40 mN/m. The increase in film compressibility because of cospread albumin indicates an inhibition of the dynamic surface activity of BLES films, i.e., larger-area reductions are needed to increase π. Cospreading BLES and albumin at the interface minimizes the adsorption barrier for PL vesicles imposed by preadsorbed albumin molecules. Therefore, the inhibitory

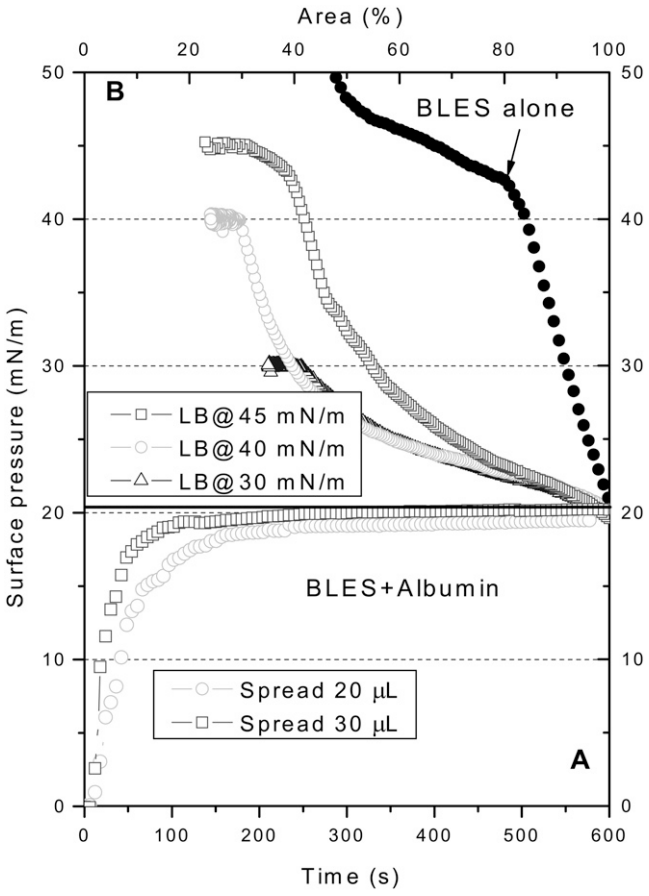

FIGURE 1 Spreading (*A*) and compression (*B*) isotherms of BLES-albumin films. Films were spread on ultrapure water from aqueous suspensions of 5 mg/mL BLES and 20 mg/mL albumin at room temperature. Spreading 20-μL samples yields a stable π of ~20 mN/m. Films were compressed at a rate of 30 mm^2/s, and were LB-transferred at 20, 30, and 40 mN/m. Spreading 30-μL samples allows LB transfer at 45 mN/m. A compression isotherm of pure BLES film spread from 20-μL 5 mg/mL BLES is shown as a reference. For reasons of comparison, this compression isotherm is shifted to the right to coincide with the initial π of the compression isotherms of BLES-albumin films.

TABLE 1 Film compressibility $(mN/m)^{-1}$ of different monolayers at various surface pressures

π	BLES	BLES + albumin	BLES + SP-A	BLES + SP-A + albumin
20	0.016 ± 0.006	0.077 ± 0.008	0.017 ± 0.006	0.078 ± 0.010
30	0.014 ± 0.002	0.044 ± 0.004	0.015 ± 0.002	0.063 ± 0.006
40	0.017 ± 0.001	0.021 ± 0.004	0.021 ± 0.003	0.035 ± 0.007

For reasons of comparison, films with or without albumin were prepared with the same amount of BLES. The BLES films were prepared using 100-μg BLES samples. The BLES films with 2.5% SP-A were prepared using 50-μg BLES samples. Four times more albumin by weight was cospread with the corresponding BLES and BLES + SP-A samples.

effect depicted in Fig. 1 may imply a new inhibition mechanism other than competitive adsorption.

Limited by mechanical design, the LWB used in this study can only reach a minimum surface area of 15–20%, which restricts the maximum π for LB transfer. To transfer LB films at π higher than 40 mN/m, 30-μL samples (i.e., 150 μg BLES + 600 μg albumin) were spread. This increased the rate at which equilibrium was attained but not the π_e of albumin, indicating that the air-water interface was already saturated with albumin when 20-μL samples were spread. With this higher spreading amount, the compression isotherms became steeper, and allowed a maximum π of 45 mN/m for LB transfer with our LWB. This π corresponds to the middle of a plateau in the compression isotherms. Further increasing the spreading amount did not significantly vary the shape of the compression isotherms (results not shown). It is worth stressing that the shape of the compression isotherms of the BLES-albumin films depends on the initial amount of spreading (20 vs. 30 μL in Fig. 1). In other words, the change in film composition (i.e., PL/albumin molecular ratio) upon compression is dependent on the initial amount of spreading. This variation in film composition of cospread films upon compression will be discussed in detail.

It should be noted that the increase in π during the compression of cospread films was mainly attributable to BLES rather than albumin. As shown in Fig. 2, adsorbed albumin films can only regulate π within a narrow range between ~20 and ~32 mN/m with the same compression rate used for BLES-albumin films.

Fig. 3, *A–D*, shows characteristic AFM images for the BLES-albumin films. At 20 mN/m (Fig. 3 *A*), the film was transferred without compression. The AFM image is of a flat, featureless pattern with a height variation of <0.1 nm. This pattern closely resembles pure albumin films at their π_e (Fig. 2, *inset*). The presence and homogeneity of albumin molecules on the mica surface were confirmed using FITC-labeled BSA (results not shown). This AFM observation is consistent with tensiometric measurements (Fig. 1 *A*), and suggests that after cospreading, the air-water interface is covered primarily by a saturated amount of albumin molecules.

It should be noted that the root mean-square roughness of AFM images in Figs. 2 and 3 *A*, measured over areas of 5 × 5 μm, is 0.18 nm and 0.19 nm, respectively. These values are lower than the roughness of human serum albumin (HSA) monolayers reported previously (43). Using the tapping mode AFM, Sheller et al. (43) measured the roughness of homogenous HSA monolayers as 0.32–0.35 nm. This difference likely arises from the different scanning modes used in these two studies. The contact-mode scanning used in our study is more susceptible to tip effects when scanning soft samples such as albumin. As a result of pressing the soft samples, the thickness and roughness measured in the contact model can be smaller than the actual values. We measured the roughness of BSA monolayers, using the tapping model, as 0.37–0.39 nm, which is close to previous measurements. Nevertheless, this artifact due to tip effects will not significantly affect our interpretations and comparisons between samples, because the contact mode was used throughout this study.

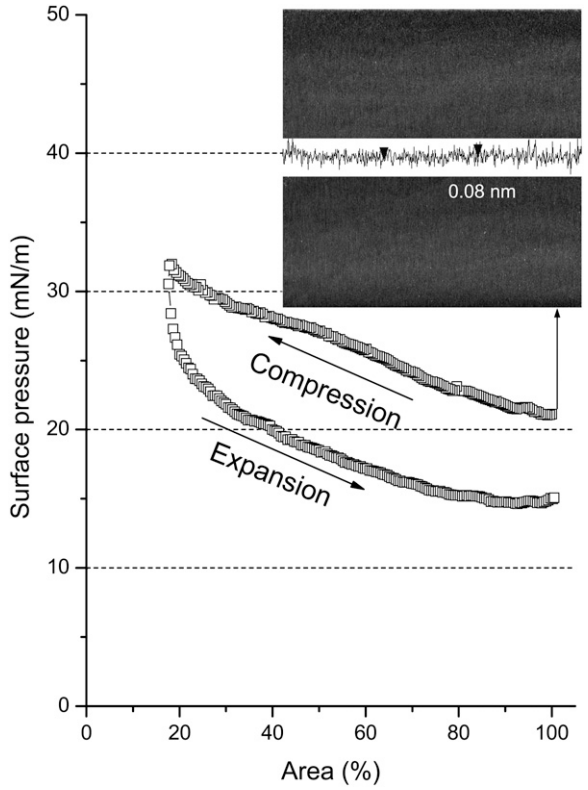

FIGURE 2 Typical compression-expansion isotherm of an adsorbed albumin film at the air-water interface. (*Inset*) Characteristic AFM topographic image (20 × 20 μm) at the equilibrium surface pressure of albumin (i.e., ~20 mN/m). The vertical distance between the two arrowheads in the cross-sectional profile is 0.08 nm.

At 30 mN/m (Fig. 3 *B*), a number of microscale hole-like domains appear. Topographic analysis revealed that both the interiors and exteriors of these domains are heterogeneous (Fig. 3 *b*). As detailed in Fig. 3 *B*, *insets*, the interiors of these domains contain grains that are 17 ± 10 nm in size and 0.7 ± 0.3 nm higher than their neighbors. The exteriors of these domains are also heterogeneous, with a height variation of up

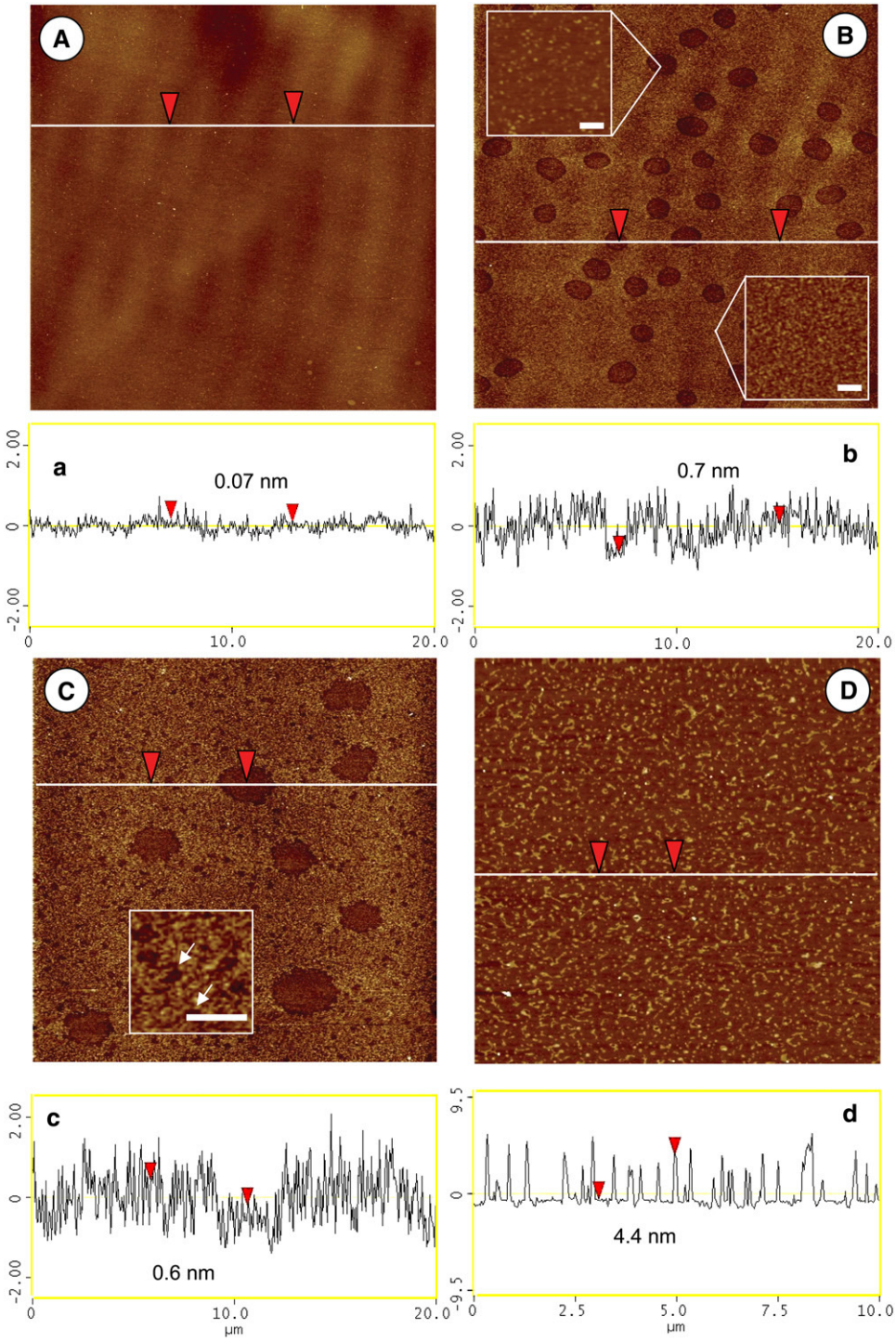

FIGURE 3 Characteristic AFM topographic images of BLES-albumin films. (*A–C*) Scan area is 20 × 20 μm. (*D*) Scan area is 10 × 10 μm. (*A*) 20 mN/m. (*B*) 30 mN/m. (*C*) 40 mN/m. (*D*) 45 mN/m. (*a–d*) Height variation along scanning line drawn in corresponding topographical image. The vertical distance between arrowheads is indicated in cross-sectional profile. (*B*, *insets*) Heterogeneity inside and outside the hole-like domains, respectively. Bars in insets represent 200 nm. (*C*, *inset*) An enlargement of nanoscale holes, indicated by arrows. Bar in inset represents 1 μm.

to 2 nm. The heterogeneity of AFM images generates difficulty in accurately estimating the depth of these domains based only on a cross-sectional analysis. (Hence, the vertical distances between arrowheads shown in the cross-sectional profiles in Figs. 3 and 5 are only indicative. The selection of arrowhead positions is neither specific nor sensitive.) Nevertheless, it appears that these domains are shallow, i.e., generally <0.5 nm lower than their surroundings. The hole-like domains cover 12% ± 3% of total surface area, slightly more than the area of microscale PL domains found in BLES monolayers at the same π (38).

At 40 mN/m (Fig. 3 *C*), the hole-like domains are destabilized, as indicated by a decrease in total domain area to 8% ± 2%. In addition, as shown in Fig. 3 *C*, *inset*, many nanoscale holes with sizes ranging from 200–300 nm appear in the film. However, because of the heterogeneity of AFM images, it

is difficult to estimate accurately the area occupied by these nanoholes.

At 45 mN/m (Fig. 3 *D*), i.e., in the plateau region of the compression isotherms (Fig. 1 *B*), multilayer structures 4.5–5.0 nm in height and ~0.1 μm in diameter are observed. These multilayers, accounting for ~1 PL bilayer stack (44), cover 16% ± 4% of the surface area.

BLES with SP-A and albumin

Fig. 4 shows the spreading (Fig. 4 *A*) and compression (Fig. 4 *B*) isotherms of BLES-albumin (1:4) films with the addition of 2.5% SP-A relative to the PL in BLES. (A compression isotherm of a representative BLES and SP-A film is also shown in Fig. 4 *B* as a reference.) Spreading 10-μL or 15-μL samples increased π to the π_e of albumin. It was found that the addition of SP-A (2.5%) cannot reverse the inhibition attributable to cospread albumin. Rather, the addition of SP-A slightly increased the film compressibility (Table 1). Increasing the SP-A to 5% and 10% did not significantly vary the film compressibility (results not shown).

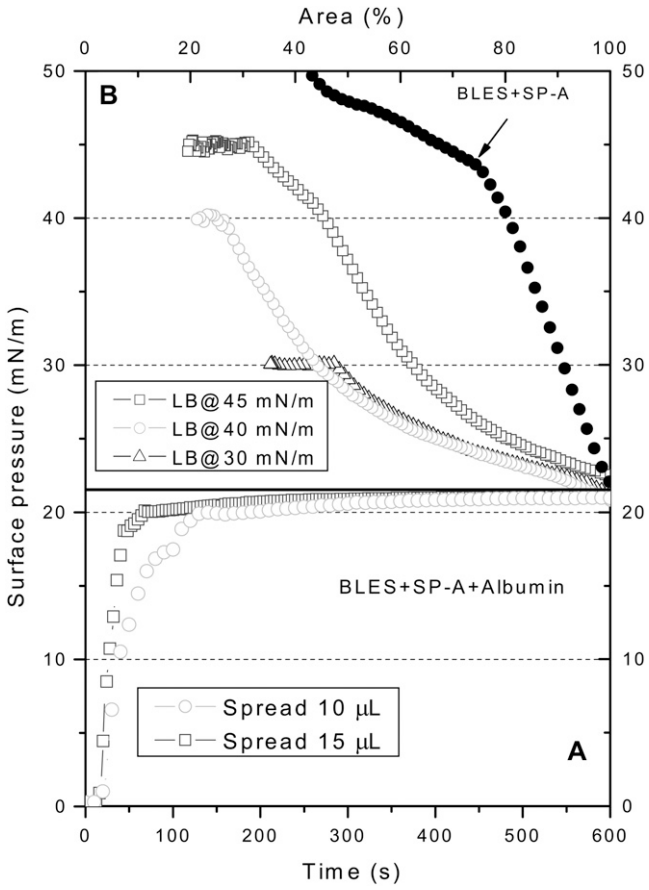

FIGURE 4 Spreading (*A*) and compression (*B*) isotherms of BLES-albumin films with SP-A. Films were spread from an aqueous suspension of 5 mg/mL BLES with 2.5% SP-A and 20 mg/mL albumin. The amounts spread were usually 10 μL, unless high deposition pressure was required. To deposit a film at 45 mN/m, 15-μL samples were spread. The subphase and rate of compression are the same as in Fig. 1. A compression isotherm of BLES and SP-A films without albumin is shown as a reference. This film was prepared by spreading 10-μL 5 mg/mL BLES with 2.5% SP-A. For reasons of comparison, this compression isotherm is shifted to the right to coincide with the initial π of the compression isotherms of the films with albumin.

Fig. 5, *A–D*, provides characteristic AFM images of BLES films with SP-A and albumin. These images are of combined features of BLES films with SP-A (38) and with albumin (Fig. 3), respectively. At 20 mN/m (Fig. 5 *A*), i.e., before film compression, the film appears to be flat and rather featureless, except for a few isolated bright (high) spots. These spots appear to be SP-A octadecamers or aggregates formed by SP-A self-association (38). At 30 mN/m (Fig. 5 *B*), hole-like domains appear with most of the domain boundaries associated with SP-A aggregates. Most of the SP-A aggregates appear at the right boundaries of these lower domains. This might indicate an artifact because of tip effects: the AFM tip dragged the SP-A aggregates down the scanning direction (from left to right), so that most of these aggregates drifted to the right and finally stuck at the boundaries of the holes. A close look at these individual SP-A aggregates revealed that they possessed diamond or rectangular shapes. This can also be attributed to artifacts because of dirty or blunt tips. Such artifacts were not previously evident when studying monolayers of BLES and SP-A (38). However, the AFM tips may be more susceptible to contamination when scanning albumin samples, because this protein can easily stick to the tips. These artifacts attributable to AFM tips do not likely alter the overall structures of the phospholipid phase separation, which is the main interest of this study.

At 40 mN/m (Fig. 5 *C*), more bright spots appear, but the majority of these seem to be squeezed out of the PL monolayer, which is consistent with our previous finding for BLES and SP-A monolayers (38). Moreover, at 40 mN/m, the originally lower hole-like domains appear to reverse their height, to become ''islands'' with a deep halo. At 45 mN/m (Fig. 5 *D*), multilayers with a maximum height of ~14 nm appear.

DISCUSSION

Albumin-induced variations in surface activity

The competitive adsorption mechanism stipulates that surfactant inhibition because of serum proteins, such as albumin, arises from the ability of these proteins to monopolize the surface, thereby impeding the adsorption or spreading of surfactant PL. Hence, this mechanism predicts that a surfactant film directly spread at an air-water interface to a particular π should not be affected by albumin, whether the protein was dissolved in the subphase or was spread at the interface (19). However, our study shows that cospread BLES-albumin films at the air-water interface are significantly inhibited, at least during the first compression (Fig. 1).

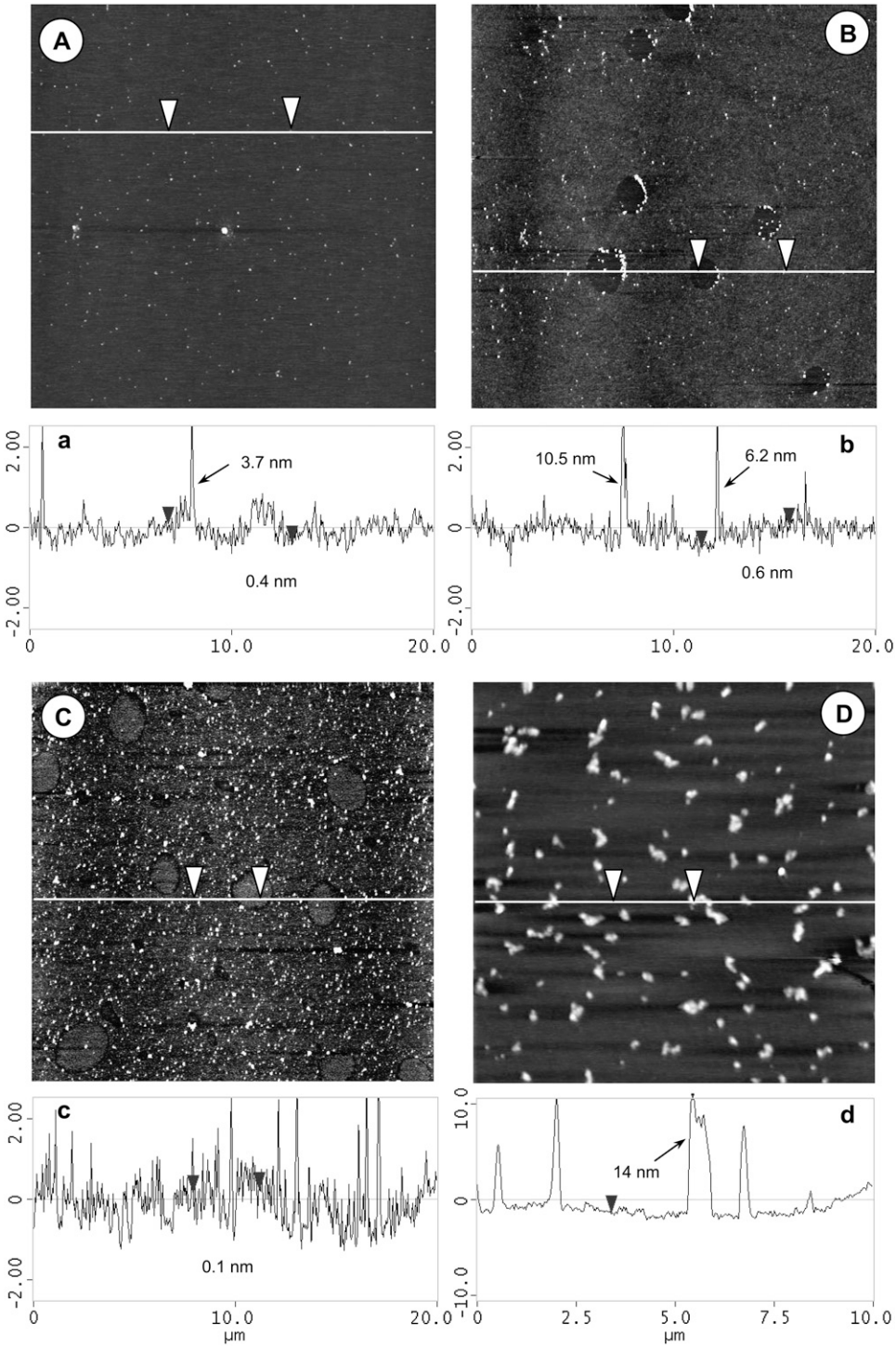

FIGURE 5 Characteristic AFM topographic images of BLES-albumin films with SP-A. (*A–C*) Scan area is 20 × 20 μm. (*D*) Scan area is 10 × 10 μm. (*A*) 20 mN/m. (*B*) 30 mN/m. (*C*) 40 mN/m. (*D*) 45 mN/m. (*a–d*) Height variation along scanning line drawn in corresponding topographical image. The vertical distance between arrowheads is indicated in cross-sectional profile. Heights of bright spots in these images vary from ~4 nm to more than 10 nm, as indicated in cross-sectional profiles.

The ability of albumin to interfere with the dynamic surface activity of BLES was further investigated with a large Langmuir trough (Nima Technology, Coventry, UK). With a larger operational surface area (~750 cm^2), this trough removes the restriction in area reduction encountered by the small trough used in Fig. 1. Therefore, more complete compression isotherms can be obtained. This trough was used to conduct multiple compression-expansion cycles of BLES-albumin (1:4) films. As shown in Fig. 6, the isotherm for the first compression reproduces that obtained using the small trough (Fig. 1 *B*). The film compressibility decreases only slightly from the first to the second compression, but remains relatively unchanged during the next five repeated compressions. This indicates that repeated compression-expansion cycles cannot counteract surfactant inhibition because of the cospread albumin. This finding is rather surprising, because

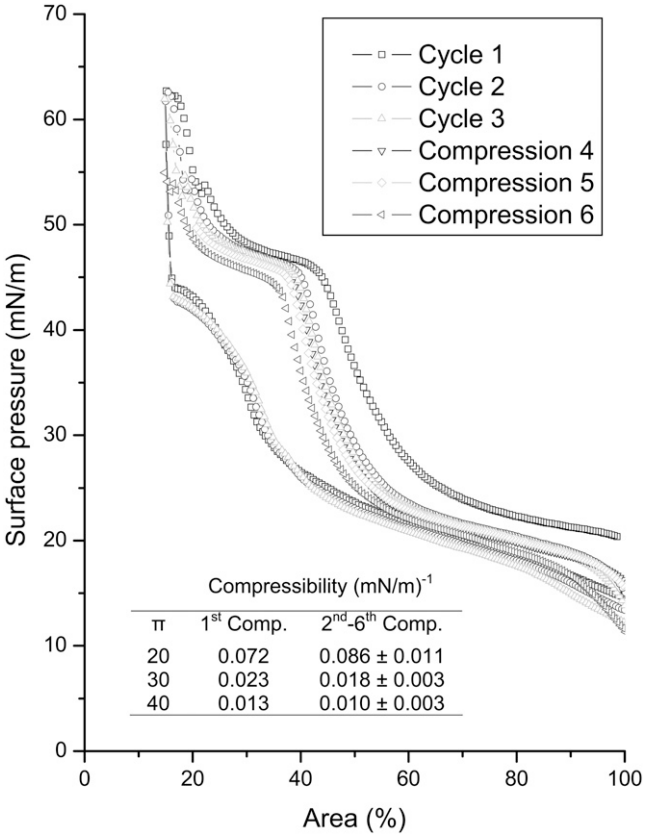

FIGURE 6 Repeated compression-expansion isotherms of a cospread BLES-albumin (1:4 w/w) film. Cycles 1–3 are shown with complete compression-expansion isotherms. Cycles 4–6 are shown with only compression branches. These experiments were conducted in a large Langmuir trough with an operational area of ~750 cm^2. The compression isotherms shifted to the left with repeated compressions, indicating loss of surface active material from the interface. Despite the shift, the shape of these compression isotherms, i.e., the film compressibility, only varied slightly with an increasing number of compressions. (*Inset*) Compressibility (*Comp.*) at 20, 30, and 40 mN/m of the first compression and the average of subsequent five compressions.

previous studies showed that albumin molecules can be removed from the air-water interface by simply overspreading a dipalmitoyl phosphatidylcholine (DPPC) monolayer (42), or by a few compression-expansion cycles when excess surfactant vesicles exist in the subphase (18).

Although inhibition is not mitigated by repeated compressions, the compressibility of BLES-albumin films decreases during each compression (Table 1 and Fig. 6). This implies a gradual refining of the films by squeezing out albumin molecules from the interface. At 40 mN/m, the compressibility of cospread films approaches that of pure BLES films, indicating nearly complete removal of albumin molecules. As shown in Fig. 6, the isotherms undergo a plateau between 40–50 mN/m, and then rise steeply after passing this plateau. This pattern closely resembles pure BLES films in the same π range (38). However, the film compressibility increases again at the onset of a subsequent compression (Fig. 6). This indicates readsorption of albumin molecules into the BLES monolayers during film expansion. Note that the π at the end of expansion, i.e., the onset of recompression, is lower than the π_e of albumin (i.e., <20 mN/m). Warriner et al. (22) showed that albumin in the subphase interferes with the readsorption and respreading of collapsed PL films at a π of 20 mN/m or lower. Our experiments further suggest that albumin molecules can remain at, or reenter, an interfacial PS film at a low π range (<40 mN/m), even though they are squeezed out at higher π. By remaining at the interface, albumin can inhibit surfactant films by increasing film compressibility. This point of view is further supported by directly imaging variations in film organization, as discussed below.

Albumin-induced variations in film organization

The albumin-induced variations in film compressibility are consistent with variations in film organization. AFM revealed two distinct variations in monolayer topography between BLES (38) and BLES-albumin films, even though the same amount of BLES was spread in both cases. First, at 20 mN/m, pure BLES monolayers showed a clear separation of tilted-condensed (TC) and liquid-expanded (LE) phases, as demonstrated by the formation of micrometer-sized TC domains (i.e., microdomains) that are generally 0.6–1.0 nm higher than the surrounding LE phase (38). In contrast, in the presence of albumin, no TC domains can be found at this π (Fig. 3 *A*). Second, when pure BLES monolayers were compressed from 30–40 mN/m, the microdomains appeared to be destabilized, as indicated by a decrease in domain area (38). Accompanying the decrease in microdomains was an increase in nanometer-sized TC domains (i.e., nanodomains) (38). The same trend in the π-dependent evolution of microdomains was found in BLES-albumin films. However, the originally higher TC domains in BLES monolayers became somewhat lower than their surroundings, and apparent heterogeneity occurred both inside and outside the domains (Fig. 3, *B* and *C*). The heterogeneity of AFM images prevented the explicit detection of any nanoscale features of the film at 30 mN/m. However, nanoholes were evident at 40 mN/m (Fig. 3 *C*), although their sizes were relatively larger than the nanodomains found in BLES monolayers (38).

Similar variations in film organization were reported by Nag et al. (33) for BLES films mixed with fetal calf serum (BLES-serum, 1:0.5 w/w). Nag et al. (33) hypothesized that the formation of hole-like domains suggested that the serum selectively interacted with the TC-phase PL, thus perturbing the lipid packing in TC domains (33). The heterogeneity of domains is also consistent with our previous studies of PS lavaged from excised rats' lungs subjected to injuriously high-stretch ventilation (45). A direct comparison of our study's BLES-albumin films with the surfactant obtained from injured lungs, however, is complicated insofar as the contents of both serum proteins and cholesterol were found to be in-

creased in the injured lungs (45). Nevertheless, it appears clear that surfactant inhibition by serum proteins is associated with variations in film organization, from a configuration in which relatively homogeneous island-like TC domains are embedded within a LE phase, into an organization where heterogeneous hole-like domains are distributed within a relatively rough matrix.

Because compressibility measurements suggested that albumin molecules can only be completely squeezed out from the interface at π higher than 40 mN/m, the variations in film organization observed at π of 20–40 mN/m may be attributed to albumin molecules remaining at the interface. To understand further the role of albumin molecules in varying the film organization, we examined BLES-albumin films with 1% FITC-labeled BSA, using fluorescence confocal microscopy (FCM) (Zeiss LSM 510). As shown in Fig. 7, FCM images of BLES-albumin films confirm that albumin remains at the interface at 30 mN/m. The dark dye-excluding domains shown in Fig. 7 are consistent with the hole-like domains revealed by AFM at the same π (Fig. 3 *B*), although with larger sizes, possibly because of the different substrates used for LB transfer.

Fig. 7 shows that albumin molecules preferentially partition into the LE phase of the BLES monolayers, which argues against specific interactions between albumin and the TC-phase PL. Hence, the manner by which albumin alters the film organization remains unknown. To address this question, we measured the absolute thicknesses of albumin and BLES monolayers by scraping away parts of the monolayers using AFM tips with a large force and a high frequency, as described by Dufrene et al. (46). The film thickness could then be determined by measuring the stepwise depth of monolayers relative to the mica surface. (A detailed description of the experimental methods can be found in the Supplementary Material, Data S1.) The thickness of albumin monolayers (at 20 mN/m) was measured to be 3.0 ± 0.5 nm, which is in good agreement with previous measurements (43,47). This value is smaller than the theoretical monomolecular dimension of albumin, when it assumes a side-on position at the interface (i.e., ~4 nm). As mentioned above, this difference could be due to an artifact, because AFM tips press soft samples, such as proteins, so that they yield smaller measurements than the actual thickness of the samples. Alternatively, this may be a consequence of albumin molecules undergoing conformational changes or structural deformations after adsorbing to the air-water interface (43). The thickness of BLES monolayers (LE phase at 30 mN/m) was measured at 2.0 ± 0.3 nm. It was reported that the thickness of DPPC bilayers in the liquid-crystalline phase is 3.7–4.3 nm, and 4.7 nm for bilayers in the gel phase (44). Accordingly, the monolayer thickness of DPPC may be approximated as 2 nm by assuming a single leaflet of these bilayers. Our AFM measurements are consistent with these data.

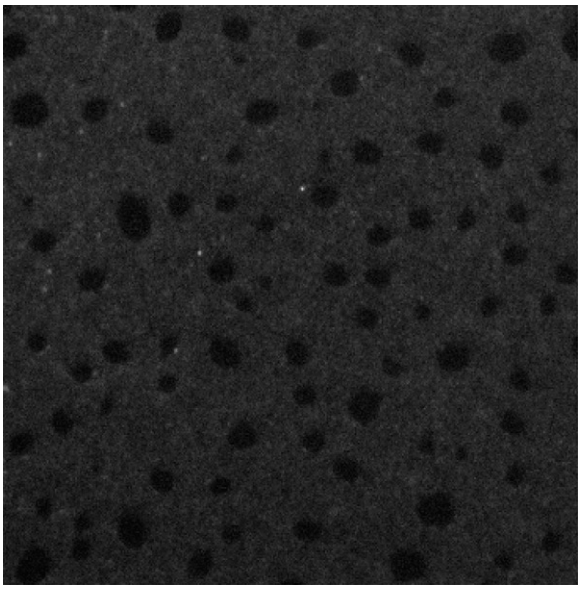

FIGURE 7 A fluorescence confocal microscopy image of BLES-albumin (1:4 w/w, with 1% FITC-labeled BSA) films. Scan area is 50 × 50 μm. Films were prepared by the same procedures as in Fig. 1. The LB films were deposited onto glass coverslips at 30 mN/m. This image demonstrates that albumin coexists with BLES within the LE phase of the monolayer at a π higher than the π_e of albumin (i.e., >20 mN/m).

Given that albumin monolayers are slightly thicker than BLES monolayers, and taking into account the tensiometric measurements (Fig. 1) and FCM observations (Fig. 7), the film organization of BLES-albumin films revealed by AFM may be explained by the diagram in Fig. 8). (Fig. 8 illustrates film organization at the air-water interface. The topographic analysis by AFM, however, was conducted on LB films transferred to solid supports.)

First, assuming a similar film incorporation efficiency, cospreading BLES-albumin 1:4 by weight would result in a mixed monolayer with a molecular ratio of ~20 PL to 1 albumin (Fig. 8 *A*). By assuming the one-dimensional molecular dimensions of PL and albumin to be 1 nm (headgroup) and 10 nm (side-on position), respectively, the molecular area ratio between PL and albumin should be ~1:100. This leads to a surface-area ratio of ~1:5 between PL and albumin after cospreading. Hence, the π of the mixed monolayer is predominantly controlled by albumin, as indicated by the rapid attainment of the π_e of albumin (~20 mN/m) after cospreading (Fig. 1 *A*). The PL molecules are expected to be in a relatively homogeneous LE phase, where the headgroups of PL molecules are translationally disordered, and the fatty-acid chains are conformationally disordered (48). This film organization results in the flat, featureless topographic characteristics observed immediately after cospreading (Fig. 3 *A*), similar to the structure of pure albumin monolayers (Fig. 2, *inset*).

Second, when π is increased beyond the π_e of albumin (~20 mN/m) but below the π_e of PL in BLES (~45 mN/m), the albumin molecules gradually leave the interface, but the PL molecules remain (Fig. 8 *B*). This results in an increased

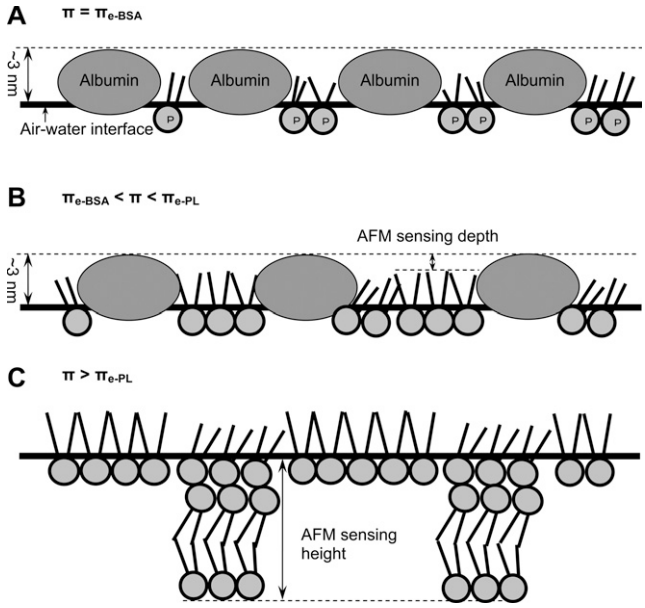

FIGURE 8 Diagram of film organization for cospread BLES and albumin films compressed at an air-water interface. Although the film organization is illustrated at the air-water interface, the topographic analysis by AFM was conducted on LB films transferred onto solid supports. The molecular dimensions of PL (labeled *P*) and albumin are not strictly scaled. (*A*) Film organization at 20 mN/m (i.e., π_e of albumin). Immediately after cospreading, the interfacial film consists of both PL and albumin at a molecular ratio of ~20:1. The PL molecules are in a conformationally disordered LE phase, and are underneath the albumin monolayer, which has a thickness of ~3 nm. Hence, AFM reveals a homogeneous film. (*B*) Film organization in the π range of ~20 to ~45 mN/m. In this π range, albumin molecules are gradually squeezed out from the interface. The PL molecules, on the other hand, increase packing density, thus undergoing the LE-TC phase transition. The TC domains consist of closely packed, disaturated PL molecules in a gel phase, excluding the albumin molecules. Hence, AFM reveals hole-like domains with low depths. Because of disturbance by albumin molecules (e.g., residual albumin trapped inside domains, or lipid-protein interactions), both the interior and exterior of these domains are topographically heterogeneous. (*C*) Film organization at π higher than ~45 mN/m (i.e., π_e of PL in BLES). In this π range, albumin molecules are largely squeezed out from the interface. The PL molecules start to form multilayered structures by partial collapse of the interfacial monolayer. Hence, AFM reveals features higher than a monomolecular thickness. Although they have been squeezed out, albumin molecules likely remain associated with the PL (not shown), because they can readily readsorb upon film expansion.

PL/albumin molecular ratio at the interface (as indicated by the decrease in film compressibility shown in Table 1). The actual PL/albumin molecular ratio at a certain π depends on the initial amount of spreading (i.e., total numbers of PL and albumin molecules at the interface before compression). Consequently, compression isotherms of BLES-albumin films spread from 20-μL and 30-μL samples, although anchored at the same initial π of 20 mN/m, show different film compressibilities (Fig. 1 *B*).

In contrast to the collapse of the albumin monolayer, the PL monolayer increases its packing density upon film compression, leading to an LE-TC phase transition similar to the phase transition of pure BLES monolayers (38). The TC domains contain disaturated PL in a gel phase that excludes hydrophobic surfactant proteins (SP-B/C) and albumin (Fig. 7). Because of the persistence of albumin molecules at the interface, the TC domains are detected as sunken holes by AFM (Fig. 3, *B* and *C*).

At π higher than 40 mN/m, nearly all albumin molecules are removed from the interface, leaving a nearly pure BLES monolayer, as indicated by the film compressibility (Table 1 and Fig. 6), as discussed above. Another indication of the removal of albumin involves the change of domain morphology from holes to islands, as observed at 40 mN/m in Fig. 5 *C*.

Third, when π is further increased beyond the π_e of the PL in BLES (~45 mN/m), the PL monolayer partially collapses to form multilayers that consist of an interfacial monolayer plus interconnected bilayers (Fig. 8 *C*) (38). The monolayer-to-multilayer transition corresponds to the plateau at 40–50 mN/m in the compression isotherms (Fig. 6) (38,49). The multilayer structures found at 45 mN/m (Fig. 3 *D*) show smaller sizes and predominantly single-bilayer thicknesses, compared with the larger sizes and multi-bilayer thicknesses of BLES films at 50 mN/m (38). This comparison confirms the growth of multilayer structures corresponding to π increase in the uprising plateau region. This is consistent with the nucleation-growth theory for the formation of compression-driven multilayers from an interfacial monolayer (i.e., two-dimensional to three-dimensional transition) (50).

Phospholipid-protein interactions: from general physicochemical studies to pulmonary surfactant inhibition

The interfacial molecular interactions between chemical surfactants and proteins in general and between PL and albumin in particular are well-documented because of their importance in many biomedical and biotechnological applications, especially in food colloidal systems (51–53). The interactions between proteins and PL monolayers are dependent on the electrostatic charges of both the lipids and the proteins and the π of monolayers.

It has long been known that proteins such as albumin can penetrate PL monolayers at low π (usually no more than 20 mN/m) (54). It was also shown microscopically that protein penetration is dependent on the phase of PL monolayers (55–57). Albumin can coexist at the interface with pure PL (such as DPPC) in the LE phase, but is squeezed out at higher π, where the PL monolayer consists of a nearly homogeneous TC phase (57). Such penetration and squeeze-out processes appear to be driven by surface energetic and steric causes, and no specific PL-protein interaction was found to be involved (56). The DPPC monolayers show LE-TC phase transition/coexistence in a narrow π range of 9–13 mN/m at room temperature (48). In contrast, condensed domains in PS films start growing at ~10 mN/m (58,59), and LE-TC phase coexistence persists at 40 mN/m (38) and likely even up to

near 70 mN/m (60). Consequently, it is expected that albumin coexists with BLES in the LE phase to a π higher than 20 mN/m (Fig. 7).

The albumin molecules remaining at the interface may suppress the normal PL phase transition in PS monolayers, because the condensed domains have to grow at the expense of compressing and displacing the protein layer. It is known that proteins such as albumin at the interface can form a strong, viscoelastic two-dimensional gel because of strong intermolecular interactions (52). Consequently, in the presence of albumin, the normal phase separation in PS films can be disturbed to some degree, especially when the protein layer is tightly packed. Evidence along this line requires further investigation.

There is evidence that once squeezed out of the interface at high π, proteins can remain associated with the lipid monolayer by electrostatic or hydrophobic binding (51,52). These attached albumin molecules or albumin-lipid complexes can be effectively adsorbed back to the surface as π decreases (51,52,61). These previous findings are in good agreement with the deleterious effects of albumin shown in Fig. 6, which were not mitigated after repeated compression-expansion cycles, although squeeze-out was evident at the high π of each compression. This view is consistent with the findings of interactions/binding between albumin and PS bilayers. Larsson et al. (31) and Nag et al. (32) showed that a small amount of albumin altered the thickness and lipid order of PL bilayers of BLES by binding tightly to the bilayers. With a better understanding of the nature of these molecular interactions, Fig. 8 could be amended accordingly to reveal the molecular interactions/binding between albumin and PL or surfactant-associated proteins (SP-B/C) in BLES.

The heterogeneity of BLES-albumin films observed here is also in good agreement with previous studies of mixed surfactant-protein films (53,57,61). For example, de Souza et al. (61) showed that addition of albumin in nanomolar concentrations can significantly increase the roughness of LB films of PL. The specific morphological variation was dependent on the charge of the PL monolayers. De Souza et al. (61) attributed the alternations in surface morphology to disturbed lipid packing because of PL-protein interactions (61).

Effect of SP-A on albumin-induced surfactant inhibition

Previous in vitro and in vivo studies demonstrated that a trace of SP-A (i.e., 1–5 wt % relative to PL) can significantly enhance the resistance of lipid extract surfactants to inhibition due to a variety of substances, including albumin (26–28). Our study, however, shows that SP-A from 2.5–10% added to 5 mg/mL BLES cannot effectively reverse the inhibition attributable to 20 mg/mL albumin (Fig. 4). The characteristic AFM images obtained with and without SP-A show a similar PL film organization (Fig. 3 versus Fig. 5). Compared with previously published data (26–28), this cannot be explained by the stoichiometric ratios between surfactant PL, albumin, and SP-A. The main difference between our work and previous studies involves the experimental design. In previous in vitro studies, SP-A was mixed with surfactant preparations and serum proteins in the subphase. In our study, however, SP-A, BLES, and albumin were spread directly at the interface. Our study thus suggests that SP-A reverses albumin-induced inhibition largely by enhancing adsorption. This view is consistent with the function of SP-A in the absence of inhibitors (38). Unless excessive PL vesicles are available in the subphase, SP-A cannot significantly enhance the dynamic surface activity of surfactant films. In fact, the direct addition of SP-A to the interface slightly increases the film compressibility (Table 1). This finding is analogous to the destabilization effects of hydrophobic surfactant proteins on PL monolayers reported by Lhert et al. (62).

Although not directly enhancing the surface activity of interfacial monolayers, SP-A appears to play a role in stabilizing multilayer structures, even in the presence of albumin. The multilayer structures formed with SP-A are ~3-fold higher than those formed without SP-A at the same π (Fig. 5 *d* versus Fig. 3 *d*). This is consistent with the ability of SP-A to promote the formation of multilayer structures in the absence of albumin (38).

Physiological relevance to ARDS

Albumin spreading or cospreading with PS is not physiologically relevant to ARDS. A more relevant experimental design would involve spreading surfactant at the interface, and injecting albumin into the subphase (16,19,22). This approach, however, would ''contaminate'' the subphase, causing technical difficulties with AFM imaging. Previous experiments using subphase injections showed that albumin in the subphase is not very effective at penetrating a preformed PS film at π above 20 mN/m (16,19,22). In healthy lungs, π likely varies between 70 mN/m to not much lower than 40 mN/m (63,64). Therefore, although it normally exists in the alveolar fluid in small amounts (39), albumin does not pose a threat under healthy conditions.

In ALI/ARDS, however, PS undergoes chemical alteration due to oxidation, or physical dilution via pulmonary edema (5,13,65). In addition, there are metabolic changes attributable to inflammation (5,13). Schmidt et al. (66) reported that the major PL and protein components of endogenous surfactant were significantly reduced in ARDS patients. The alveolar contents of DPPC, SP-A, SP-B, and SP-C were all reduced to ~50% of healthy controls, and these levels recovered only slowly and incompletely during 8 days of observation (66). Significantly reduced surface activity was associated with this compositional degradation (66). Under these conditions, albumin penetration could occur at the most energetically favorable sites of impaired PS films, e.g., those places with decreased film thickness, reduced lipid packing, and altered electrical surface potential (14).

In conclusion, this study suggests a new biophysical mechanism for surfactant inhibition by serum proteins, such as albumin. Albumin remains in the LE phase of surfactant monolayers at π up to 40 mN/m, i.e., much higher than the π_e of albumin (~20 mN/m). By mixing and coexisting with PL at the interface, albumin increases film compressibility. Hence, a much greater reduction in area is required to achieve high π (i.e., low surface tensions). Although albumin molecules are squeezed out of the interface at higher π, they may remain associated with the interface in such a way that they can readily readsorb with decreasing π. Consequently, this inhibitory effect of albumin cannot be readily relieved by repeated compression-expansion cycles. It must be stressed that this new mechanism of surfactant inhibition does not necessarily contradict other inhibition mechanisms attributable to serum proteins, such as competitive adsorption. Instead, it complements the competitive adsorption mechanism by addressing an additional deleterious effect of albumin molecules once they enter the interface, a condition that is likely in ALI/ARDS. It was also found that SP-A cannot effectively counteract this inhibitory effect, indicating that SP-A reverses surfactant inhibition primarily by enhancing PL adsorption, rather than by directly altering lipid packing at the interface.

SUPPLEMENTARY MATERIAL

To view all of the supplemental files associated with this article, visit www.biophysj.org.

We thank Dr. Lijuan Yao for isolating SP-A, and BLES Biochemicals for the generous donation of BLES. We also thank Prof. Peter Norton (University of Western Ontario) for the use of the Zeiss confocal microscope, and Prof. Elmar Prenner (University of Calgary) for the use of the Nima Langmuir trough.

This work was supported by Operating Grants MOP-64406 and FRN-15462 from the Canadian Institutes of Health Research. Y.Y.Z. is grateful for Postdoctoral Fellowship PDF-328777-200 from the Natural Sciences and Engineering Research Council of Canada.

REFERENCES

1. Notter, R. H. 2000. Lung Surfactants. Basic Science and Clinical Applications. Marcel Dekker, Inc., New York.
2. Martin, J. A., B. E. Hamilton, P. D. Sutton, S. J. Ventura, F. Menacker, and M. L. Munson. 2003. Births: final data for 2002. *Natl. Vital Stat. Rep.* 52:1–113.
3. Ware, L. B., and M. A. Matthay. 2000. The acute respiratory distress syndrome. *N. Engl. J. Med.* 342:1334–1349.
4. McIntyre, R. C., Jr., E. J. Pulido, D. D. Bensard, B. D. Shames, and E. Abraham. 2000. Thirty years of clinical trials in acute respiratory distress syndrome. *Crit. Care Med.* 28:3314–3331.
5. Griese, M. 1999. Pulmonary surfactant in health and human lung diseases: state of the art. *Eur. Respir. J.* 13:1455–1476.
6. Frerking, I., A. Gunther, W. Seeger, and U. Pison. 2001. Pulmonary surfactant: functions, abnormalities and therapeutic options. *Intensive Care Med.* 27:1699–1717.
7. Robertson, B., and H. L. Halliday. 1998. Principles of surfactant replacement. *Biochim. Biophys. Acta.* 1408:346–361.
8. Schoendorf, K. C., and J. L. Kiely. 1997. Birth weight and age-specific analysis of the 1990 US infant mortality drop. Was it surfactant? *Arch. Pediatr. Adolesc. Med.* 151:129–134.
9. Guyer, B., M. A. Freedman, D. M. Strobino, and E. J. Sondik. 2000. Annual summary of vital statistics: trends in the health of Americans during the 20th century. *Pediatrics.* 106:1307–1317.
10. Gregory, T. J., K. P. Steinberg, R. Spragg, J. E. Gadek, T. M. Hyers, W. J. Longmore, M. A. Moxley, G. Z. Cai, R. D. Hite, R. M. Smith, L. D. Hudson, C. Crim, P. Newton, B. R. Mitchell, and A. J. Gold. 1997. Bovine surfactant therapy for patients with acute respiratory distress syndrome. *Am. J. Respir. Crit. Care Med.* 155:1309–1315.
11. Lewis, J. F., and R. Veldhuizen. 2003. The role of exogenous surfactant in the treatment of acute lung injury. *Annu. Rev. Physiol.* 65: 613–642.
12. Baudouin, S. V. 2004. Exogenous surfactant replacement in ARDS:–one day, someday, or never? *N. Engl. J. Med.* 351:853–855.
13. Gunther, A., C. Ruppert, R. Schmidt, P. Markart, F. Grimminger, D. Walmrath, and W. Seeger. 2001. Surfactant alteration and replacement in acute respiratory distress syndrome. *Respir. Res.* 2:353–364.
14. Zuo, Y. Y., R. A. Veldhuizen, A. W. Neumann, N. O. Petersen, and F. Possmayer. 2008. Current perspectives in pulmonary surfactant—inhibition, enhancement and evaluation. *Biochim. Biophys. Acta.* 10.1016/j.bbamem.2008.1003.1021.
15. Gunasekara, L., S. Schurch, W. M. Schoel, K. Nag, Z. Leonenko, M. Haufs, and M. Amrein. 2005. Pulmonary surfactant function is abolished by an elevated proportion of cholesterol. *Biochim. Biophys. Acta.* 1737:27–35.
16. Holm, B. A., Z. Wang, and R. H. Notter. 1999. Multiple mechanisms of lung surfactant inhibition. *Pediatr. Res.* 46:85–93.
17. Tabak, S. A., and R. H. Notter. 1977. Effect of plasma proteins on the dynamic [pi]—a characteristics of saturated phospholipid films. *J. Colloid Interface Sci.* 59:293–300.
18. Holm, B. A., R. H. Notter, and J. N. Finkelstein. 1985. Surface property changes from interactions of albumin with natural lung surfactant and extracted lung lipids. *Chem. Phys. Lipids.* 38:287–298.
19. Holm, B. A., G. Enhorning, and R. H. Notter. 1988. A biophysical mechanism by which plasma proteins inhibit lung surfactant activity. *Chem. Phys. Lipids.* 49:49–55.
20. Taeusch, H. W., J. B. de la Serna, J. Perez-Gil, C. Alonso, and J. A. Zasadzinski. 2005. Inactivation of pulmonary surfactant due to serum-inhibited adsorption and reversal by hydrophilic polymers: experimental. *Biophys. J.* 89:1769–1779.
21. Zasadzinski, J. A., T. F. Alig, C. Alonso, J. B. de la Serna, J. Perez-Gil, and H. W. Taeusch. 2005. Inhibition of pulmonary surfactant adsorption by serum and the mechanisms of reversal by hydrophilic polymers: theory. *Biophys. J.* 89:1621–1629.
22. Warriner, H. E., J. Ding, A. J. Waring, and J. A. Zasadzinski. 2002. A concentration-dependent mechanism by which serum albumin inactivates replacement lung surfactants. *Biophys. J.* 82:835–842.
23. Stenger, P. C., and J. A. Zasadzinski. 2007. Enhanced surfactant adsorption via polymer depletion forces: a simple model for reversing surfactant inhibition in acute respiratory distress syndrome. *Biophys. J.* 92:3–9.
24. Seeger, W., C. Grube, A. Gunther, and R. Schmidt. 1993. Surfactant inhibition by plasma proteins: differential sensitivity of various surfactant preparations. *Eur. Respir. J.* 6:971–977.
25. Zuo, Y. Y., H. Alolabi, A. Shafiei, N. Kang, Z. Policova, P. N. Cox, E. Acosta, M. L. Hair, and A. W. Neumann. 2006. Chitosan enhances the in vitro surface activity of dilute lung surfactant preparations and resists albumin-induced inactivation. *Pediatr. Res.* 60:125–130.
26. Cockshutt, A. M., J. Weitz, and F. Possmayer. 1990. Pulmonary surfactant-associated protein A enhances the surface activity of lipid extract surfactant and reverses inhibition by blood proteins in vitro. *Biochemistry.* 29:8424–8429.
27. Venkitaraman, A. R., S. B. Hall, J. A. Whitsett, and R. H. Notter. 1990. Enhancement of biophysical activity of lung surfactant extracts and

phospholipid-apoprotein mixtures by surfactant protein A. *Chem. Phys. Lipids.* 56:185–194.

28. Sun, B., T. Curstedt, G. Lindgren, B. Franzen, A. A. Alaiya, A. Calkovska, and B. Robertson. 1997. Biophysical and physiological properties of a modified porcine surfactant enriched with surfactant protein A. *Eur. Respir. J.* 10:1967–1974.
29. Taeusch, H. W., K. W. Lu, J. Goerke, and J. A. Clements. 1999. Nonionic polymers reverse inactivation of surfactant by meconium and other substances. *Am. J. Respir. Crit. Care Med.* 159:1391–1395.
30. Gunasekara, L., W. M. Schoel, S. Schurch, and M. W. Amrein. 2008. A comparative study of mechanisms of surfactant inhibition. *Biochim. Biophys. Acta.* 1778:433–444.
31. Larsson, M., T. Nylander, K. M. Keough, and K. Nag. 2006. An x-ray diffraction study of alterations in bovine lung surfactant bilayer structures induced by albumin. *Chem. Phys. Lipids.* 144:137–145.
32. Nag, K., K. M. Keough, and M. R. Morrow. 2006. Probing perturbation of bovine lung surfactant extracts by albumin using DSC and 2H-NMR. *Biophys. J.* 90:3632–3642.
33. Nag, K., A. Hillier, K. Parsons, and M. F. Garcia. 2007. Interactions of serum with lung surfactant extract in the bronchiolar and alveolar airway models. *Respir. Physiol. Neurobiol.* 157:411–424.
34. Seeger, W., G. Stohr, H. R. Wolf, and H. Neuhof. 1985. Alteration of surfactant function due to protein leakage: special interaction with fibrin monomer. *J. Appl. Physiol.* 58:326–338.
35. Yamada, T., M. Ikegami, B. L. Tabor, and A. H. Jobe. 1990. Effects of surfactant protein-A on surfactant function in preterm ventilated rabbits. *Am. Rev. Respir. Dis.* 142:754–757.
36. Yukitake, K., C. L. Brown, M. A. Schlueter, J. A. Clements, and S. Hawgood. 1995. Surfactant apoprotein A modifies the inhibitory effect of plasma proteins on surfactant activity in vivo. *Pediatr. Res.* 37:21–25.
37. Bruni, R., B. R. Fan, R. David-Cu, H. W. Taeusch, and F. J. Walther. 1996. Inactivation of surfactant in rat lungs. *Pediatr. Res.* 39:236–240.
38. Zuo, Y. Y., E. Keating, L. Zhao, S. M. Tadayyon, R. A. Veldhuizen, N. O. Petersen, and F. Possmayer. 2008. Atomic force microscopy studies of functional and dysfunctional pulmonary surfactant films, I: Micro- and nanostructures of functional pulmonary surfactant films and the effect of SP-A. *Biophys. J.* 94:3549–3564.
39. Ishizaka, A., T. Matsuda, K. H. Albertine, H. Koh, S. Tasaka, N. Hasegawa, N. Kohno, T. Kotani, H. Morisaki, J. Takeda, M. Nakamura, X. Fang, T. R. Martin, M. A. Matthay, and S. Hashimoto. 2004. Elevation of KL-6, a lung epithelial cell marker, in plasma and epithelial lining fluid in acute respiratory distress syndrome. *Am. J. Physiol. Lung Cell. Mol. Physiol.* 286:L1088–L1094.
40. Cruz, A., and J. Perez-Gil. 2007. Langmuir films to determine lateral surface pressure on lipid segregation. *Methods Mol. Biol.* 400:439–457.
41. Walters, R. W., R. R. Jenq, and S. B. Hall. 2000. Distinct steps in the adsorption of pulmonary surfactant to an air- liquid interface. *Biophys. J.* 78:257–266.
42. Wen, X. Y., and E. I. Franses. 2001. Adsorption of bovine serum albumin at the air/water interface and its effect on the formation of DPPC surface film. *Colloids Surf. A Physicochem. Eng. Asp.* 190:319–332.
43. Sheller, N. B., S. Petrash, M. D. Foster, and V. V. Tsukruk. 1998. Atomic force microscopy and x-ray reflectivity studies of albumin adsorbed onto self-assembled monolayers of hexadecyltrichlorosilane. *Langmuir.* 14:4535–4544.
44. Marsh, D. 1990. CRC Handbook of Lipid Bilayers. CRC Press, Boca Raton, FL.
45. Panda, A. K., K. Nag, R. R. Harbottle, K. Rodriguez-Capote, R. A. Veldhuizen, N. O. Petersen, and F. Possmayer. 2004. Effect of acute lung injury on structure and function of pulmonary surfactant films. *Am. J. Respir. Cell Mol. Biol.* 30:641–650.
46. Dufrene, Y. F., W. R. Barger, J. B. D. Green, and G. U. Lee. 1997. Nanometer-scale surface properties of mixed phospholipid monolayers and bilayers. *Langmuir.* 13:4779–4784.
47. Lu, J. R., T. J. Su, and J. Penfold. 1999. Adsorption of serum albumins at the air/water interface. *Langmuir.* 15:6975–6983.
48. Kaganer, V. M., H. Mohwald, and P. K. Dutta. 1999. Structure and phase transitions in Langmuir monolayers. *Rev. Mod. Phys.* 71:779–819.
49. Leonenko, Z., S. Gill, S. Baoukina, L. Monticelli, J. Doehner, L. Gunasekara, F. Felderer, M. Rodenstein, L. M. Eng, and M. Amrein. 2007. An elevated level of cholesterol impairs self-assembly of pulmonary surfactant into a functional film. *Biophys. J.* 93:674–683.
50. Vollhardt, D. 2006. Nucleation in monolayers. *Adv. Colloid Interface Sci.* 123–126:173–188.
51. Mackie, A. R. 2004. Structure of adsorbed layers of mixtures of proteins and surfactants. *Curr. Opin. Colloid Interface Sci.* 9:357–361.
52. MacKie, A., and P. Wilde. 2005. The role of interactions in defining the structure of mixed protein-surfactant interfaces. *Adv. Colloid Interface Sci.* 117:3–13.
53. Rodriguez Patino, J. M., M. R. Rodriguez Nino, and C. Carrera Sanchez. 2007. Physico-chemical properties of surfactant and protein films. *Curr. Opin. Colloid Interface Sci.* 12:187–195.
54. Quinn, P., and R. M. Dawson. 1970. The penetration of serum albumin into phospholipid monolayers of different fatty acid chain length and interfacial charge. *Biochem. J.* 119:21–25.
55. Zhang, H., X. Wang, G. Cui, and J. Li. 2000. Stability investigation of the mixed DPPC/protein monolayer at the air-water interface. *Colloids Surf. A Physicochem. Eng. Aspect.* 175:77–82.
56. Zhao, J., D. Vollhardt, G. Brezesinski, S. Siegel, J. Wu, J. B. Li, and R. Miller. 2000. Effect of protein penetration into phospholipid monolayers: morphology and structure. *Colloids Surf. A Physicochem. Eng. Aspects.* 171:175–184.
57. Wang, X., Y. Zhang, J. Wu, M. Wang, G. Cui, J. Li, and G. Brezesinski. 2002. Dynamical and morphological studies on the adsorption and penetration of human serum albumin into phospholipid monolayers at the air/water interface. *Colloids Surf. B Biointerfaces.* 23:339–347.
58. Discher, B. M., K. M. Maloney, W. R. Schief, Jr., D. W. Grainger, V. Vogel, and S. B. Hall. 1996. Lateral phase separation in interfacial films of pulmonary surfactant. *Biophys. J.* 71:2583–2590.
59. Nag, K., J. Perez-Gil, M. L. Ruano, L. A. Worthman, J. Stewart, C. Casals, and K. M. Keough. 1998. Phase transitions in films of lung surfactant at the air-water interface. *Biophys. J.* 74:2983–2995.
60. Piknova, B., W. R. Schief, V. Vogel, B. M. Discher, and S. B. Hall. 2001. Discrepancy between phase behavior of lung surfactant phospholipids and the classical model of surfactant function. *Biophys. J.* 81:2172–2180.
61. de Souza, N. C., W. Caetano, R. Itri, C. A. Rodrigues, O. N. Oliveira, Jr., J. A. Giacometti, and M. Ferreira. 2006. Interaction of small amounts of bovine serum albumin with phospholipid monolayers investigated by surface pressure and atomic force microscopy. *J. Colloid Interface Sci.* 297:546–553.
62. Lhert, F., W. Yan, S. C. Biswas, and S. B. Hall. 2007. Effects of hydrophobic surfactant proteins on collapse of pulmonary surfactant monolayers. *Biophys. J.* 93:4237–4243.
63. Schurch, S., J. Goerke, and J. A. Clements. 1978. Direct determination of volume- and time-dependence of alveolar surface tension in excised lungs. *Proc. Natl. Acad. Sci. USA.* 75:3417–3421.
64. Schurch, S. 1982. Surface tension at low lung volumes: dependence on time and alveolar size. *Respir. Physiol.* 48:339–355.
65. Lewis, J. F., R. Veldhuizen, F. Possmayer, W. Sibbald, J. Whitsett, R. Qanbar, and L. McCaig. 1994. Altered alveolar surfactant is an early marker of acute lung injury in septic adult sheep. *Am. J. Respir. Crit. Care Med.* 150:123–130.
66. Schmidt, R., P. Markart, C. Ruppert, M. Wygrecka, T. Kuchenbuch, D. Walmrath, W. Seeger, and A. Guenther. 2007. Time-dependent changes in pulmonary surfactant function and composition in acute respiratory distress syndrome due to pneumonia or aspiration. *Respir. Res.* 8:55.